ARL-TR-9568 ● SEP 2022

DEVCOM ARMY RESEARCH LABORATORY

Electrified Dynamic Tensile Extrusion of Hemispherical Nose Aluminum Projectiles

by Matthew J Coppinger, Brian L Wilmer, Colby T Adams, and Robert W Borys Jr

NOTICES

Disclaimers

The findings in this report are not to be construed as an official Department of the Army position unless so designated by other authorized documents.

Citation of manufacturer's or trade names does not constitute an official endorsement or approval of the use thereof.

Destroy this report when it is no longer needed. Do not return it to the originator.

ARL-TR-9568 ● SEP 2022

Electrified Dynamic Tensile Extrusion of Hemispherical Nose Aluminum Projectiles

Matthew J Coppinger, Colby T Adams, and Robert W Borys Jr
DEVCOM Army Research Laboratory

Brian L Wilmer
SURVICE Engineering

REPORT DOCUMENTATION PAGE

Form Approved
OMB No. 0704-0188

1. REPORT DATE *(DD-MM-YYYY)*	2. REPORT TYPE	3. DATES COVERED (From - To)
September 2022	Technical Report	1 May 2019–8 June 2022

4. TITLE AND SUBTITLE
Electrified Dynamic Tensile Extrusion of Hemispherical Nose Aluminum Projectiles

5a. CONTRACT NUMBER

5b. GRANT NUMBER

5c. PROGRAM ELEMENT NUMBER

6. AUTHOR(S)
Matthew J Coppinger, Brian L Wilmer, Colby T Adams, and Robert W Borys Jr

5d. PROJECT NUMBER

5e. TASK NUMBER

5f. WORK UNIT NUMBER

7. PERFORMING ORGANIZATION NAME(S) AND ADDRESS(ES)
DEVCOM Army Research Laboratory
ATTN: FCDD-RLW-TA
Aberdeen Proving Ground, MD 21005

8. PERFORMING ORGANIZATION REPORT NUMBER
ARL-TR-9568

9. SPONSORING/MONITORING AGENCY NAME(S) AND ADDRESS(ES)

10. SPONSOR/MONITOR'S ACRONYM(S)

11. SPONSOR/MONITOR'S REPORT NUMBER(S)

12. DISTRIBUTION/AVAILABILITY STATEMENT
Approved for public release: distribution unlimited.

13. SUPPLEMENTARY NOTES
ORCID ID: Robert Borys, 0000-0002-3616-9663

14. ABSTRACT
The use of electrification to increase the velocity enhancement of aluminum projectiles during dynamic tensile extrusion is explored. Experiments were performed in both electrified and unelectrified configurations with impact velocities between 475 and 575 m/s. Photon Doppler velocimetry was used to determine velocities, and X-ray radiography and optical shadowgraphy were used for imaging. Specimen breakup times are discussed and the percentage increases in velocity for the lead particles are presented.

15. SUBJECT TERMS
DTE, pulsed power, PDV, shadowgraphy, aluminum, Terminal Effects

16. SECURITY CLASSIFICATION OF:			17. LIMITATION OF ABSTRACT	18. NUMBER OF PAGES	19a. NAME OF RESPONSIBLE PERSON
a. REPORT	b. ABSTRACT	c. THIS PAGE			Matthew J Coppinger
Unclassified	Unclassified	Unclassified	UU	30	19b. TELEPHONE NUMBER (Include area code) (410) 278-0185

Contents

List of Figures

List of Tables

Acknowledgments

The authors would like to thank Mr Jeffrey Ball for experimental assistance at Experimental Facility 167, Drs W Casey Uhlig and Paul Berning for consultation on the electrified experiments, and Dr Michael Zellner for support with the photon Doppler velocimetry system.

1. Introduction

High-velocity and hypervelocity phenomena are an area of interest for the US Army Combat Capabilities Development Command Army Research Laboratory. Applications that are relevant to the US Army range from laboratory high-velocity tools for material response analysis to complex protection and lethality concepts. Recent research involved a laboratory miniature electrothermal (ET) launcher for millimeter-sized projectiles.[1–5] Compact laboratory devices have significant value for subscale material analysis given their potential for high-throughput data acquisition and ease of operation. For such devices to generate as complete a set of data as possible, a broad range of operational velocities is desirable. Already the miniature millimeter-sized projectile launcher developed at DEVCOM Army Research Laboratory has demonstrated velocities in excess of 4000 m/s.[4] Extending this range to higher velocities will prove beneficial for studies that explore high-velocity interactions in a table-top configuration.

A material response evaluation technique known as dynamic tensile extrusion (DTE) is one interesting candidate to further increase the velocity of a moving projectile. DTE is an experimental technique used to explore material response in tension under high strains and high strain rates.[6] DTE involves launching a spherical or hemispherical nose specimen through a conical reducing die at a sufficient velocity to result in high strain and high-strain-rate conditions. Intense pressure is generated in the specimen as it impacts the die allowing the material to flow, and the velocity at the front of the specimen increases to conserve mass flow as the cross-sectional area of the die is reduced.

Velocity increases during DTE have been documented for metals including Cu and Zr.[7–9] The use of a restricting die to interact with low-strength sabots has also been investigated as a means of increasing the velocity of a projectile.[10] Trujillo et al. noted a "tensile pullback" during DTE extrusion.[7] The tensile pullback can result in the entire specimen arresting in the die if the material is not stressed to failure; however, if the impact velocity is high enough to cause the material to fracture, the lead particles proceed at elevated velocities.[9] In addition, temperature can affect the DTE of a specimen. Particles from Zr specimens that were extruded at elevated temperatures experienced greater elongation than room-temperature samples.[8] Hydrocode simulations have also indicated that specimens extruded at higher temperatures can undergo a greater increase in velocity.[11]

The present study explores the possibility of using DTE to increase the velocity of Al projectiles for relevant applications such as a millimeter-size launcher. The prospect of achieving an additional enhancement in velocity from increasing the

specimen temperature as it extrudes is also explored. Typically, DTE specimens are heated inductively prior to firing to achieve a uniform temperature distribution. In this work, rather than heating the sample prior to launching the specimen, DTE specimens are ohmically heated during the extrusion process with high electrical currents. Electrified DTE is fitting for applications that might benefit from heated specimens but that require rapid response times. The technique is uniquely suitable for electromagnetic launch where substantial currents are already part of the device operation. In addition, this work will serve to supply a set of data that can be used to validate advanced magnetohydrocodes such as ALEGRA.[12]

2. Experimental Setup

During the development of the ET gun, Al was recognized as a suitable material for high-velocity projectiles.[1] As a result, projectiles for this study were fashioned from extruded rods of Al 6061-T6511. Rods were machined to a length of 20 mm with a hemispherical nose on one end and a diameter of 6.35 mm. The length of 20 mm was chosen so that the electrodes in electrified experiments could be separated sufficiently for the voltages needed, yet still allow current to flow when the projectile completed the circuit. Projectiles were accelerated to between 475 and 575 m/s using a powder gun. This velocity range was sufficient to allow necking and particulation in both the unelectrified and electrified samples. Reducing dies were fabricated from A10 tool steel with a 10° half angle, and experiments were conducted at Experimental Facility (EF) 167 in air to assess their impact in applications that might require similar ambient conditions.

The electrified DTE concept is illustrated in Fig. 1a. Projectiles were fired through a brass sleeve that was slightly wider than the projectile and in contact with a ground electrode. Shortly thereafter, the projectiles impacted the extrusion die, which was in contact with the high-voltage electrode. Clearance between the projectile and the brass sleeve was kept under 1 mm to remain small enough that the air would electrically breakdown to allow the initiation of current flow without interfering with the trajectory of the projectile. Electrical current begins flowing slightly before the projectile impacts the die when either the projectile is close enough to the die to cause electrical breakdown of the air or debris from the barrel in front of the projectile creates a conductive path.

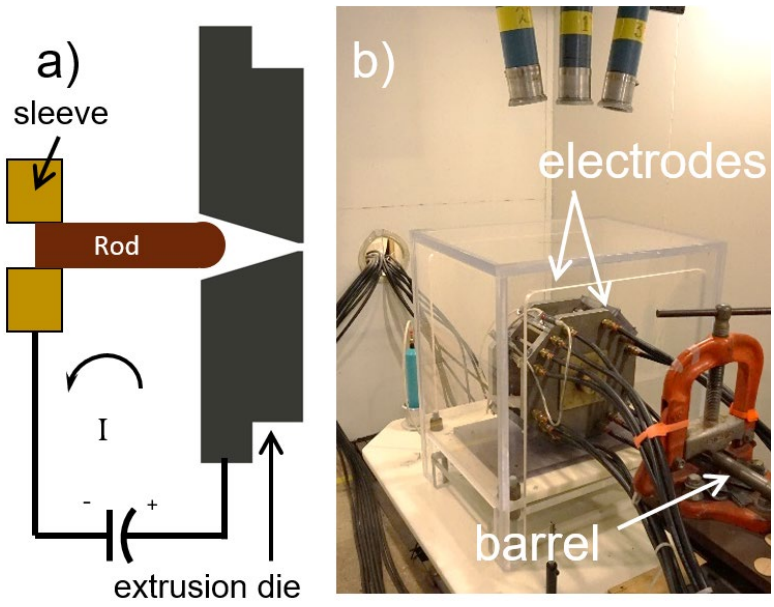

Fig. 1 a) Schematic showing the principle of electrified DTE and b) the experimental fixture showing relative locations of the barrel and electrodes

In order to pass large electrical currents through a projectile as it impacted an extrusion die, electrical current was supplied by a capacitor bank. Sixteen RG217 cables connected the capacitor bank to two octagonal electrodes (visible in Fig. 1b). For the electrified experiments, the 1.4-mF capacitor bank was charged to 6 kV, resulting in an energy storage of 25.2 kJ that delivered a peak current of nominally 300 kA to the specimens as they underwent deformation.

One additional challenge presented by the electrified concept is that the initial arc from the capacitor discharge generated broadband emission intense enough to saturate the detectors of high-speed (HS) cameras directly imaging the process. Thus, X-ray radiography was used to examine the morphology of the extruding Al specimens. The radiographic imaging presented further challenges since Al is a relatively low-density metal and exact timing was complicated by the fact the experimental setup was not outfitted with real-time velocity analysis. For consistency, X-ray radiography was employed to image both the electrified and unelectrified shots.

Velocity was primarily determined using photon Doppler velocimetry (PDV). In the unelectrified experiments, a breakscreen served as the trigger for the PDV system and the X-rays. In the electrified experiments, the signal from a calibrated Rogowski probe served as a trigger for the electrical data, the PDV system, and the X-rays.

An attempt was also made to image the final electrified shot presented here using a HS camera with laser illumination. A pulsed CAVILUX Smart laser unit illuminator was used to backlight the extruding specimen while a synchronized Shimadzu HPV X2 camera recorded images. This combination was previously demonstrated to generate quantitative information in pulse power experiments.[13] The intention was to explore the possibility that an intense monochromatic light source might be able to capture some of the process via shadowgraphy even in the presences of a broad-spectrum arc.

3. Velocity Analysis and Electrical Characteristics

PDV measurements yielded velocity data from five unelectrified DTE experiments and two electrified DTE experiments that clearly indicated the impact velocity of the incoming specimen and the velocity of the lead particle after extrusion. Unelectrified shots are designated U1–U5 while the electrified shots are designated E1 and E2.

Figure 2 shows representative spectrograms from one unelectrified experiment and one electrified experiment (additional spectrograms are included in Appendix A). In the unelectrified experiment, a breakscreen placed 89 mm from the face of the die served as the trigger for the X-rays and the PDV. Inspection of the unelectrified spectrogram (Fig. 2a) indicates the projectile impacts the die approximately 202 μs after the trigger. The projectile impact velocity was 517 m/s, and the lead particle was observed 28.15 μs later traveling at 1533 m/s. Unfortunately, debris generated during the firing and extrusion processes serve as an obscurant and add a significant degree of uncertainly to the interpretation of the PDV data during the extrusion process. Similar features are evident in the spectrogram for the electrified extrusion process (Fig. 2b). A Rogowski coil served as the trigger for the electrified experiments, so the initial impact occurs only 16 μs after the trigger. In the case of the electrified experiment, the initial projectile velocity was 537 m/s, and the lead particle was observed to have achieved a stable velocity of 1639 m/s 27.2 μs later. Interestingly, although much of the extrusion process is again obscured, the final portion of the "tensile pullback" does appear to be evident in the spectrogram.

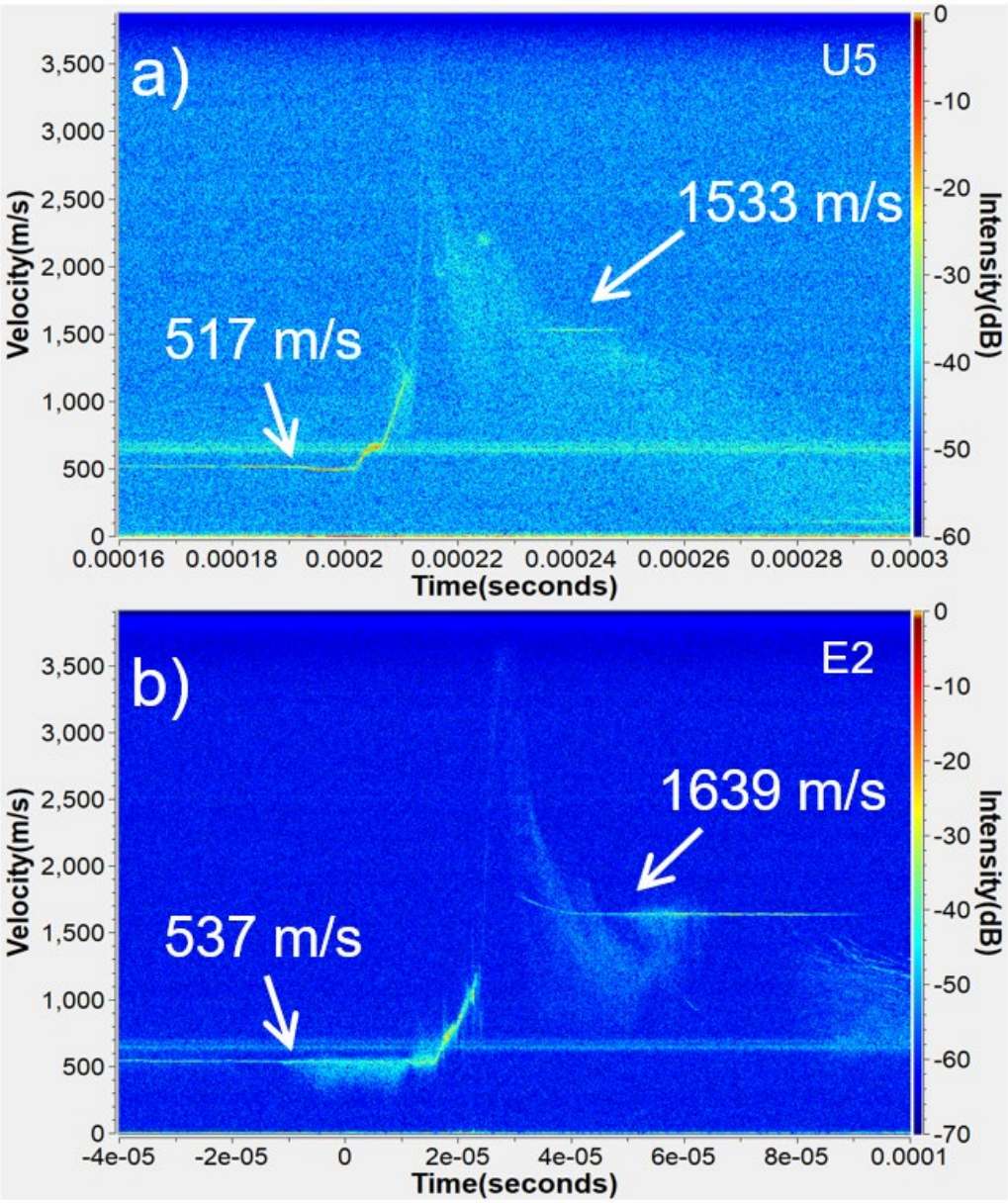

Fig. 2 a) PDV spectrogram from an unelectrified DTE experiment with an initial velocity of 517 m/s and a final velocity of 1533 m/s, and b) PDV spectrogram from an electrified DTE experiment with an initial velocity of 537 m/s and a final velocity of 1639 m/s

During the extrusion process a velocity gradient forms along the specimen. The PDV spectrograms suggest that particle velocity stabilizes when it separates from the contiguous portion of the specimen. After particulation, velocity changes little on the timescales of interest here and any slight reduction in velocity can reasonably be attributed to aerodynamic drag. For the purposes of comparison with the imaging in the following section, the breakup or particulation time is estimated from the PDV spectrograms as the time at which the velocity of the lead particle has stabilized. In three of the PDV spectrograms, the end of the tensile pullback before

stabilization was captured; therefore, a measurement of the time the velocity stabilized was made for those experiments as an estimate of the time the lead particle separated.

Velocity results for each experiment and the breakup times estimated from the three PDV spectrograms mentioned previously are summarized in Table 1. Initial velocities for the experiments ranged from 483 to 562 m/s, and velocities of the lead particles ranged from 1142 to 1700 m/s. Percentage increases of the lead particle above the initial velocities are also included. The highest velocity unelectrified experiment and both electrified experiments had percentage increases in excess of 200%, or, in other words, the lead particle for these experiments exited at more than three times the initial velocity.

Table 1 Impact velocities of projectiles, the resultant velocity lead particle, the percentage increase of the lead particle above the initial velocity, and the breakup times of the specimen (when measurement was possible).

Shot	Impact velocity (m/s)	Lead particle velocity (m/s)	Percentage increase (%)	Breakup time (μs)
U1	537	1442	168.5	. . .
U2	562	1700	202.5	. . .
U3	483	1357	181.0	24.90
U4	551	1651	199.6	. . .
E1	505	1534	203.8	20.70
U5	517	1533	196.5	. . .
E2	537	1639	205.2	27.20

The percentage increase is plotted versus the incoming velocity in Fig. 3. The unelectrified shot with an impact velocity of 537 m/s appears to deviate markedly from the trend observed in the other unelectrified data. The X-ray images from this experiment indicated that the extruded particles drifted off the shot axis, which could have been caused by an asymmetric impact with the die. This datum was therefore omitted in the linear fit to the unelectrified experiments shown as a dashed red line in Fig. 3. The fit to the unelectrified data serves as a visual indicator of the velocity enhancement that might be expected for a particular projectile impact velocity in unelectrified DTE experiments. Notably, both of the electrified experiments showed velocity increases placing them above the fit to the unelectrified experiments. This suggests that the additional velocity increases for the electrified cases are attributable to electrification during the extrusion process as opposed to simply differences in the incoming velocity. One other interesting feature shown in this plot is that the velocity enhancement in the electrified experiments does not increase as rapidly as the unelectrified cases. Although more

experimental data would be needed for confirmation, this would be consistent with the fact that a higher-velocity projectile will interact with the die for a shorter duration and will therefore be subjected to electrical current flow for a shorter amount of time.

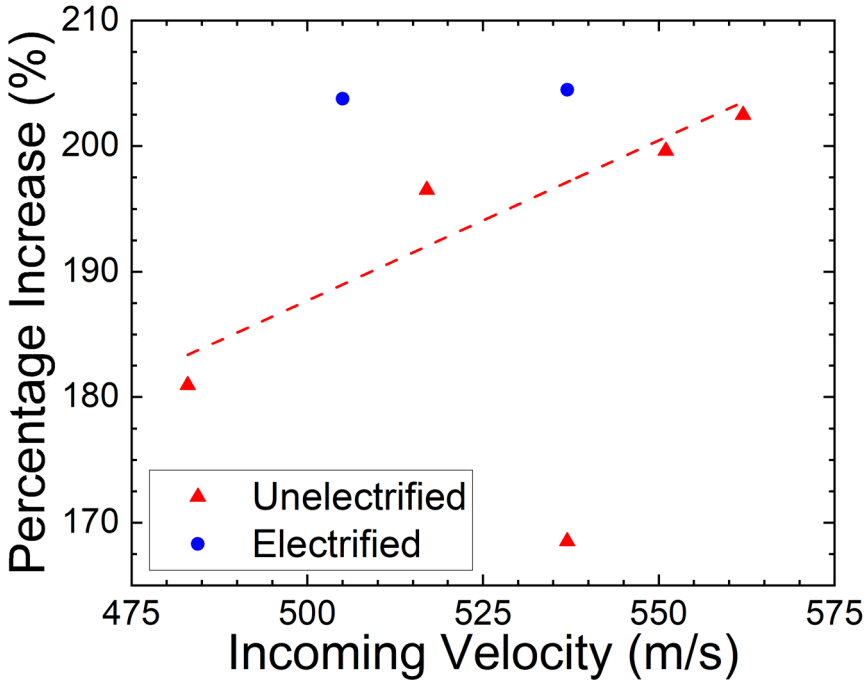

Fig. 3 The percentage increases of each unelectrified experiment (red triangles) compared to the percentage increases of the electrified experiments (blue circles)

For the two electrified experiments, the signal from the calibrated Rogowski probe was numerically integrated to yield the electrical current supplied to the specimen during extrusion. The peak current for shot E1 was 315.4 kA and the peak current for shot E2 was 301.4 kA. The current and a fit to the data from E2 are shown in Fig 4. LRC circuit parameters from the fit to the integrated data showed a decent match for a system inductance of 300 nH and a resistance of approximately 6 mΩ.

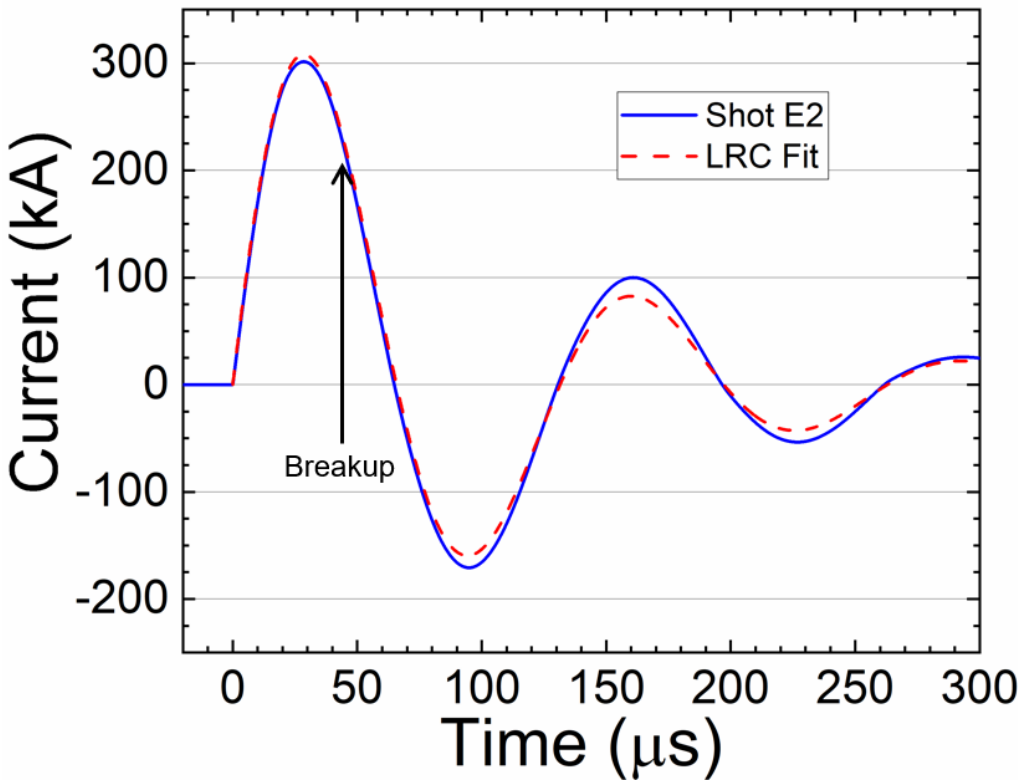

Fig. 4 Current trace and LRC fit of eletrified shot E2

An estimate of the breakup time relative to the initiation of current flow is also indicated in Fig. 4. Most of the extrusion process occurs well before this time so a relatively brief portion of the electrical discharge contributes to the ohmic heating of the sample. On these time scales, the skin effect confines higher current densities—and therefore regions of highest ohmic heating—to the outside of the specimen. Given that the resistance is dynamically changing during deformation and the temperature in the specimen is not uniform during the extrusion process, extensive analysis of the influence of ohmic heating on the material flow during extrusion is a study that is very well suited for magnetohydrocodes. Such a study is underway and will be reported in a future manuscript.

4. Imaging Results

Images of the specimens a short time after they impacted the die provide a means to examine the morphology of the process. Additionally, the time at which the specimen had already separated into individual particles could also be confirmed from these images. The morphology of an extruded specimen and the particulation time are valuable to understanding material failure and can also serve as useful metrics for code validation.

Figure 5a shows X-ray images from a representative unelectrified experiment with an impact velocity of 517 m/s, and Fig. 5b shows images from a representative electrified experiment with an impact velocity of 537 m/s. Time annotations on the images in this section are measured relative to the time of impact, which was determined from the PDV data as the time at which the projectile velocity begins to increase. X-ray timing for the unelectrified cases was complicated by the fact that the velocity was estimated before the shot. As a result, the earliest X-ray image (not shown) for shot U5 (Fig. 5a) was captured while the specimen was still inside the extrusion die. In the unelectrified case, the first X-ray captured a contiguous specimen at 25.8 μs and a particulated specimen at 47.8 μs. These images are consistent with the observation from the PDV data of a lead particle with a steady velocity 28.15 μs after impact. These times also suggest that the X-ray image at 25.8 μs was taken just before the lead particle separates. Similarly, in the electrified case for shot E2 (Fig. 5b), the first X-ray image captures a contiguous specimen at 20.28 μs and a particulated specimen at 31.59 μs. The PDV spectrogram for shot E2 indicated that a steady velocity was achieved 27.20 μs after impact which is also consistent with these X-ray images.

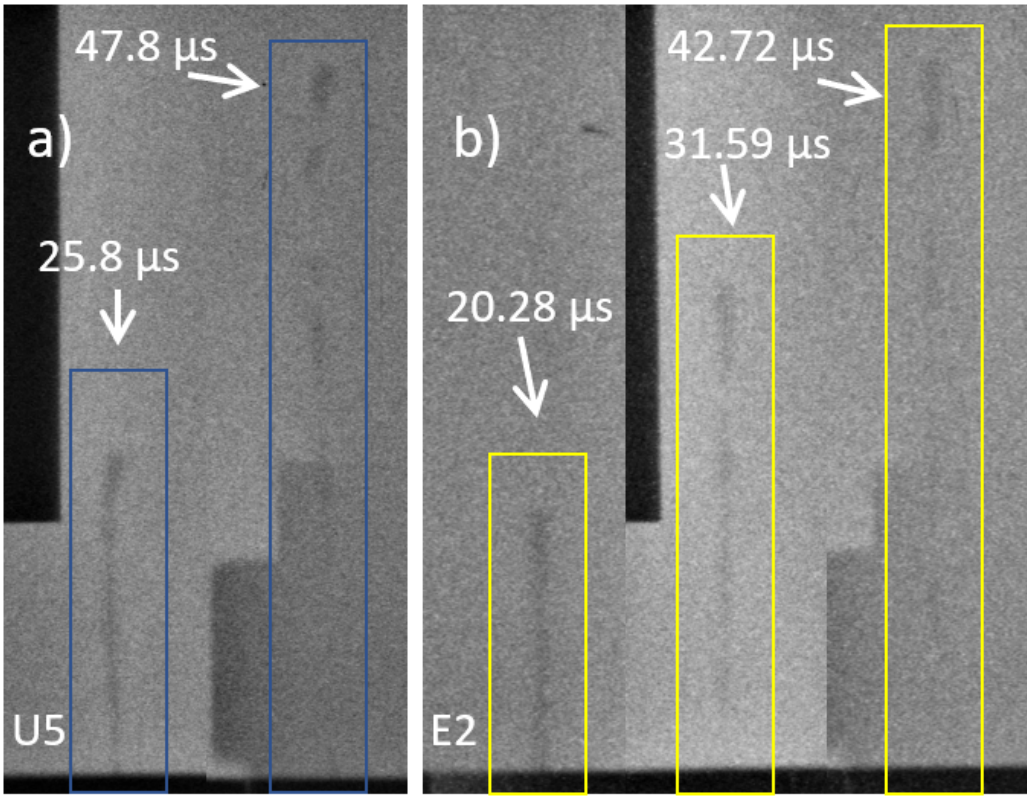

Fig. 5 X-ray images of a) unelectrified DTE experiment U5 and b) electrified DTE experiment E2

Additional imagery was captured by a HS camera for electrified experiment E2 using a pulsed laser to backlight the specimen after it exited the extrusion die. Individual frames from the video are shown in Fig. 6 in 4-μs increments. Again, image times are measured from the impact time as determined from PDV data. Debris can be observed in these images in front of the extruding specimen. This debris was partly responsible for obscuring the PDV signal during the extrusion and complicates the measurement of a velocity of the lead particle from these images. Another estimate of the specimen breakup time, however, can be obtained from these images. Recall that a steady velocity for the lead particle was observed at 27.20 μs. The 28.7-μs frame in Fig. 6 shows severe necking near the front of the specimen as the material fails and the lead particle separates. The steady velocity criterion, therefore, does appear to be a reasonable estimate of the breakup time for these specimens. The 32.7-μs frame is a very close match to the second X-ray image in Fig. 5b. In both images, the separation of a second particle is evident. The additional frames show further breakup consistent with the final X-ray image in Fig. 5b.

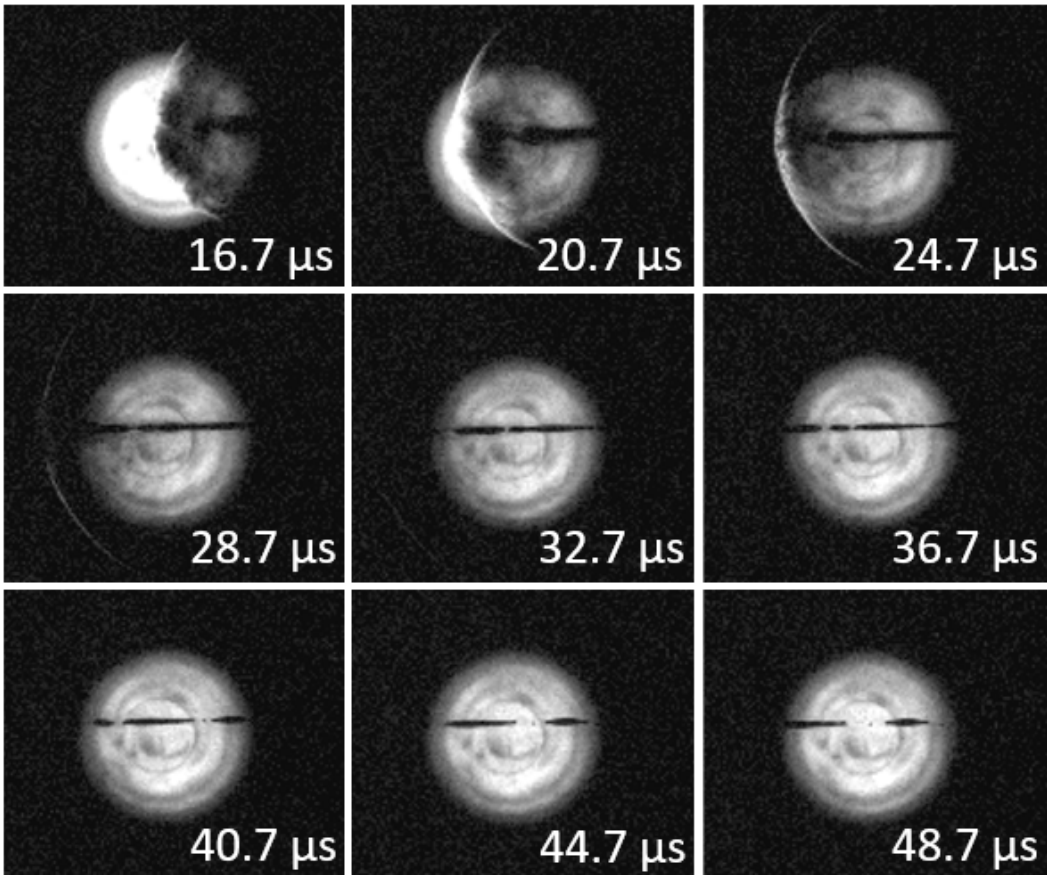

Fig. 6 Individual frames of electrified DTE from a Shimadzu backlit by a pulsed laser

Although the debris in front of the extruding specimen increases the difficulty of locating the foremost point, a frame-by-frame velocity analysis can still be attempted, and since the HS video and PDV system shared a trigger signal, they were already temporally correlated. Figure 7 shows the velocity data as determined from both the HS video and the PDV. The black solid line is a fit to the spectrogram shown in Fig. 2b. Only portions of the PDV spectrum with a high signal-to-noise ratio were used in the fit to ensure a high level of confidence that the velocity shown was that of the extruding specimen and not of the preceding debris. The blue circles are the individual frame-by-frame velocity measurements from analysis of the HS video images. There is significant spread in this data that can be attributed to the uncertainty determining the precise location of the front of the specimen; however, there is an indication that statistical methods can be employed to give a decent approximation of the velocity. The blue solid curve shows a five-point central moving average of the individual HS video data points. This curve more closely matches the velocity recorded by the PDV system. Thus, in addition to providing images of the electrified extrusion process, the backlit HS video has additional value as a means to corroborate the experimental velocity data.

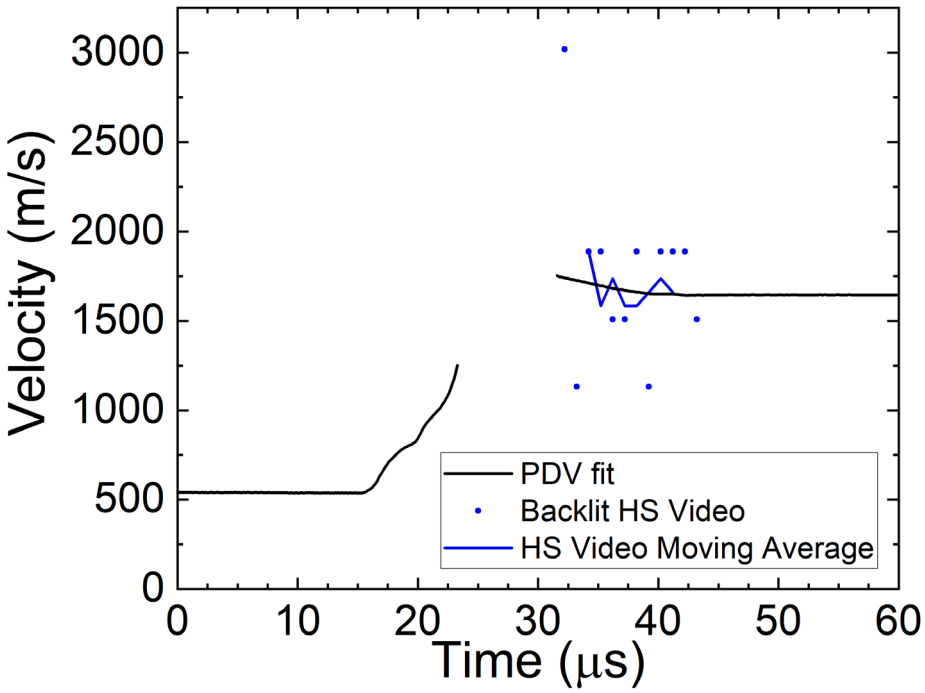

Fig. 7 Velocities of the lead particle as determined from the PDV spectrogram (black) and the backlit HS video (blue)

5. Conclusion

In summary, experiments investigating the velocity enhancement that occurs as hemispherical nose Al projectiles undergo dynamic tensile extrusion were conducted at ARL EF 167. Electrified and unelectrified experiments were conducted, and particulation and velocity enhancement were observed for specimens that impacted a die with velocities between 475 and 575 m/s. In both cases, lead particles maintained the velocity enhancement after separation. The velocity of the lead particles from electrified experiments were in excess of what might be expected from an unelectrified experiment; however, overall additional gains from the two electrified experiments as a percentage of the impact velocity were a somewhat modest 7.5% and 15% above a comparable unelectrified expectation. Therefore, this concept will certainly prove beneficial for applications where large currents are already present such as an ET gun, but it will likely have limited impact as a means to heat a sample for material analysis. The data presented here will also allow comparative analysis for the validation of magnetohydrocodes.

6. References

1. Bartkowski P, Berning P, Uhlig W, Coppinger MJ. Electrical arc driven hypersonic projectiles. CCDC Army Research Laboratory; 2019. Report No.: ARL-TR-8683.

2. Uhlig WC, Bartkowski PT, Berning PR, Coppinger MJ. Controlling chamber expansion in miniature electrothermal guns for increased velocity and efficiency. CCDC Army Research Laboratory; 2019. Report No.: ARL-TR-8722.

3. Uhlig WC, Coppinger MJ, Berning PR, Bartkowski P. Overcoming erroneous erosion of electrically launched projectiles in ALEGRA simulations. CCDC Army Research Laboratory; 2020. Report No.: ARL-TR-8888.

4. Uhlig WC, Berning PR, Bartkowski PT, Coppinger MJ. Electrically-launched mm-sized hypervelocity projectiles. Int J Impact Eng. 2020;137:103441.

5. Wilmer BL, Uhlig WC, Berning PR, Coppinger MJ. Optimizing performance of compact hypervelocity electrothermal guns: electrode composition and bore diameter. Proceedings of the 2022 Hypervelocity Impact Symposium: HVIS 2022. Forthcoming 2022.

6. Gray GT III, Cerreta EK, Yablinsky CA, Addessio LB, Henrie BL, Sencer BH, Burkett MW, Maudlin PJ, Maloy SA, Trujillo CP, Lopez MF. Influence of shock prestraining and grain size of the dynamic tensile extrusion response of copper: experiments and simulation. AIP Conference Proceedings. 2006;845:725–728.

7. Trujillo CP, Martinez DT, Burkett MW, Escobedo JP, Cerreta E, Gray GT III. A novel use of PDV for an integrated small scale test platform. AIP Conference Proceedings. 2012;1426:406.

8. Escobedo JP, Cerreta E, Martinez DT, Trujillo CP, Lebensohn RA, Gray GT III. Influence of temperature on the dynamic tensile behavior of zirconium. Metall Mater Trans A. 2014;45:5877–5882.

9. Burkett, MW. Eulerian hydrocode modeling of a dynamic tensile extrusion experiment. Proceedings of the 2019 Hypervelocity Impact Symposium; 2019.

10. Anderson WW, Jensen BJ, Cherne FJ, Owens CT, Ramos KJ, Lieber MA. Enhancing impact velocity with shock interactions in a restricting die. J Phys: Conf Ser. 2014;500:142001.

11. Coppinger, MJ. A parametric analysis of dynamic tensile extrusion using ALEGRA. DEVCOM Army Research Laboratory. Forthcoming 2022.

12. Robinson AC, Brunner TA, Carroll S, Drake R, Garasi CJ, Gardiner T, Haill T, Hanshaw H, Hensinger D, Labreche D, et al. ALEGRA: an arbitrary Lagrangian-Eulerian multimaterial, multiphysics code. Proceedings of the 46th AIAA Aerospace Sciences Meeting; 2008. Paper AIAA-2008-1235.

13. Wilmer BL, Coppinger MJ, Uhlig WC. High-speed video of electric arcs and exploding wires. CCDC Army Research Laboratory (US); 2020. Report No.: ARL-TN-1007.

Appendix. Photon Doppler Velocimetry (PDV) Spectrograms and X-ray Images

Shot U1

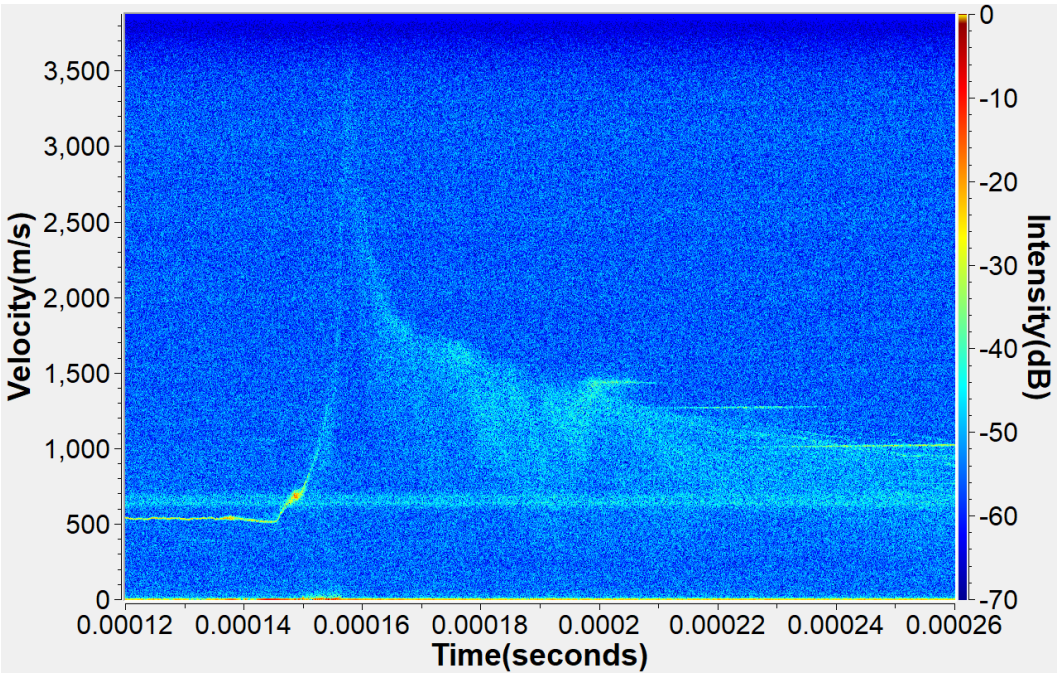

Fig. A-1 The photon Doppler velocimetry (PDV) spectrogram from unelectrified dynamic tensile extrusion (DTE) experiment U1 with an impact velocity of 537 m/s and a lead particle velocity of 1442 m/s

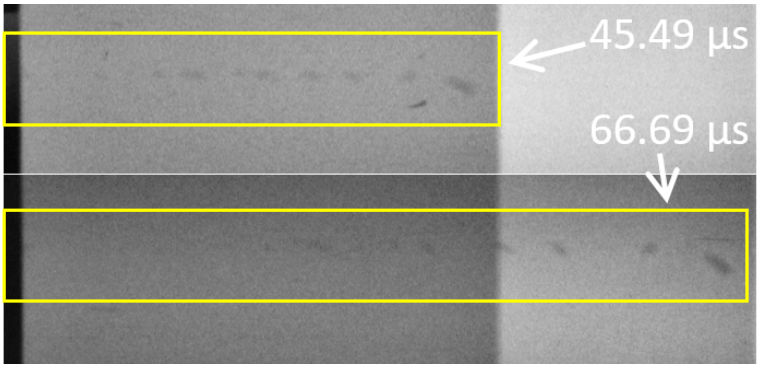

Fig. A-2 X-ray images of unelectrified DTE experiment U1. Times are measured relative to impact.

Shot U2

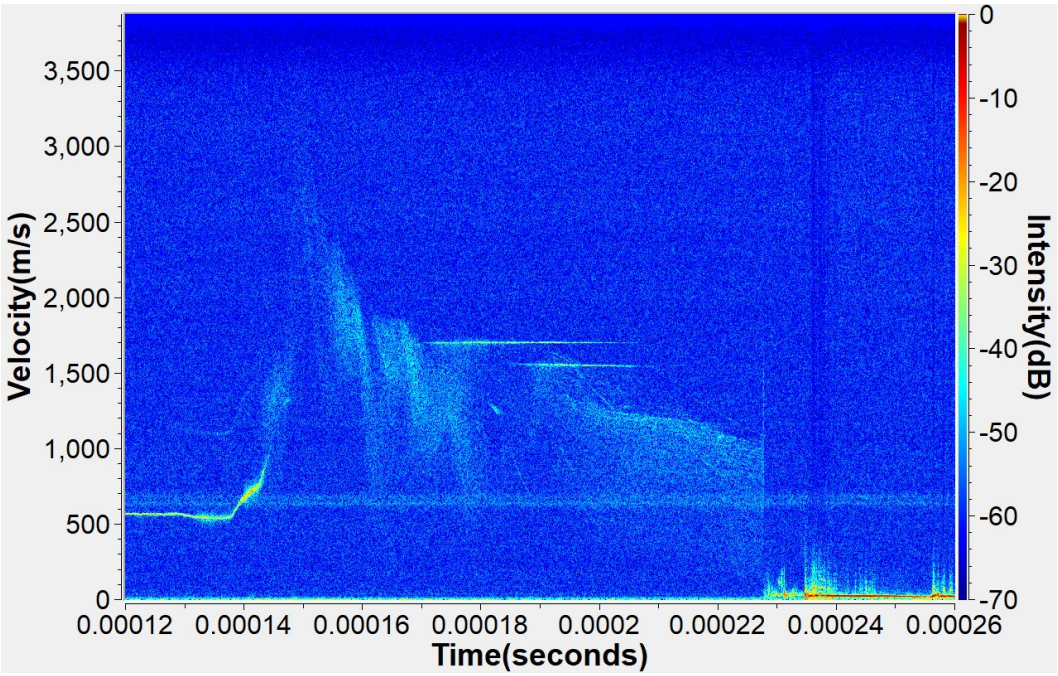

Fig. A-3 The PDV spectrogram from unelectrified DTE experiment U2 with an impact velocity of 562 m/s and a lead particle velocity of 1700 m/s

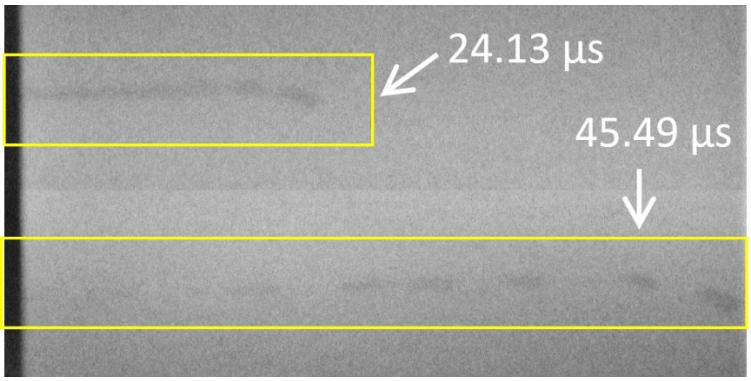

Fig. A-4 X-ray images of unelectrified DTE experiment U2. Times are measured relative to impact.

Shot U3 (no X-ray images available)

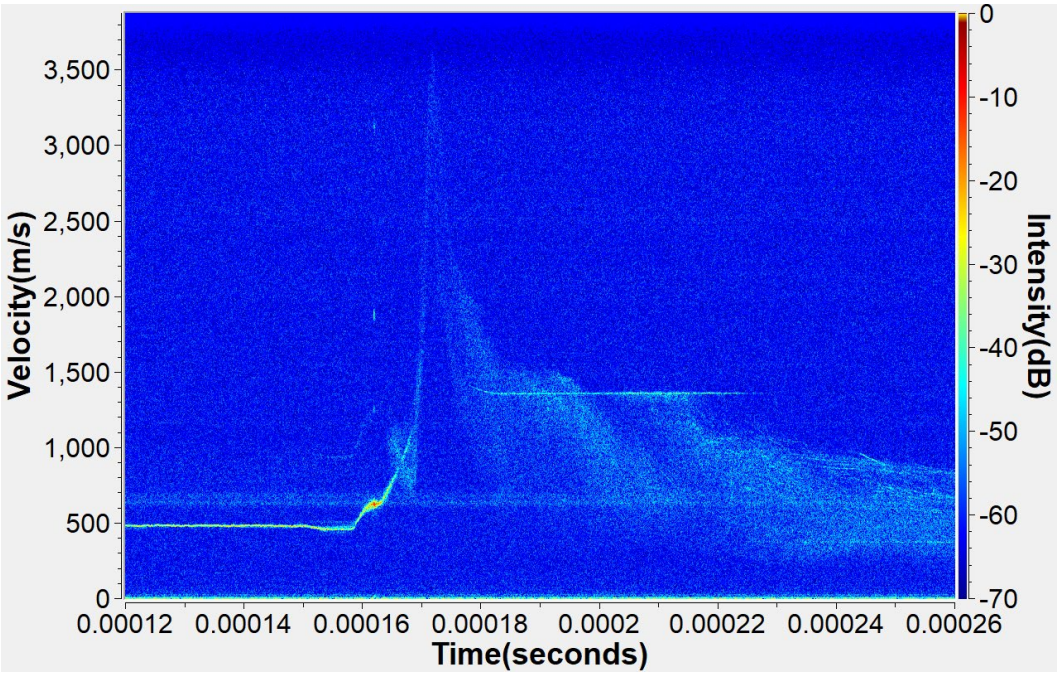

Fig. A-5 The PDV spectrogram from unelectrified DTE experiment U3 with an impact velocity of 483 m/s and a lead particle velocity of 1357 m/s

Shot U4

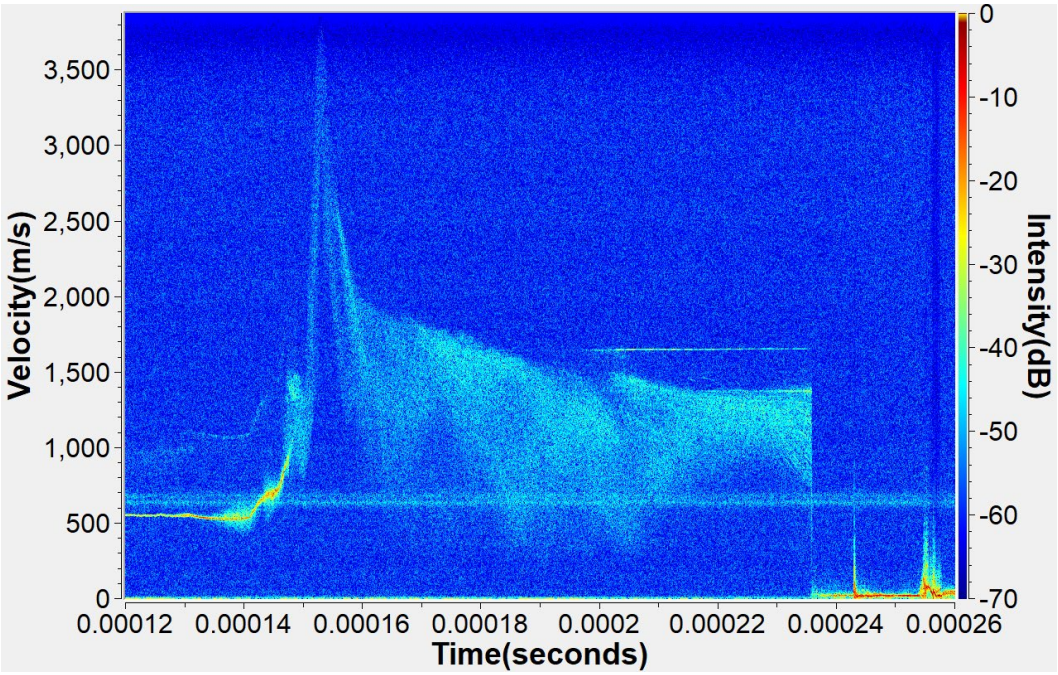

Fig. A-6 The PDV spectrogram from unelectrified DTE experiment U4 with an impact velocity of 551 m/s and a lead particle velocity of 1651 m/s

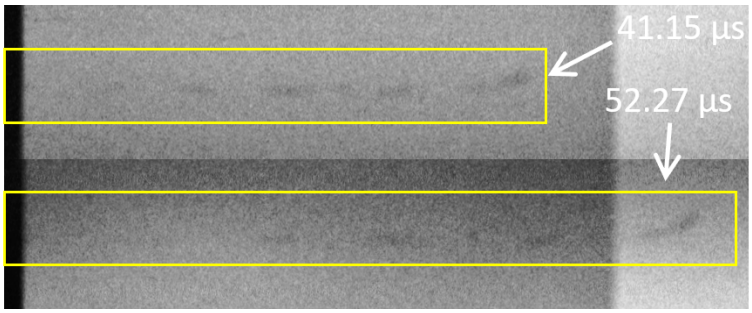

Fig. A-7 X-ray images of unelectrified DTE experiment U4. Times are measured relative to impact.

Shot E1

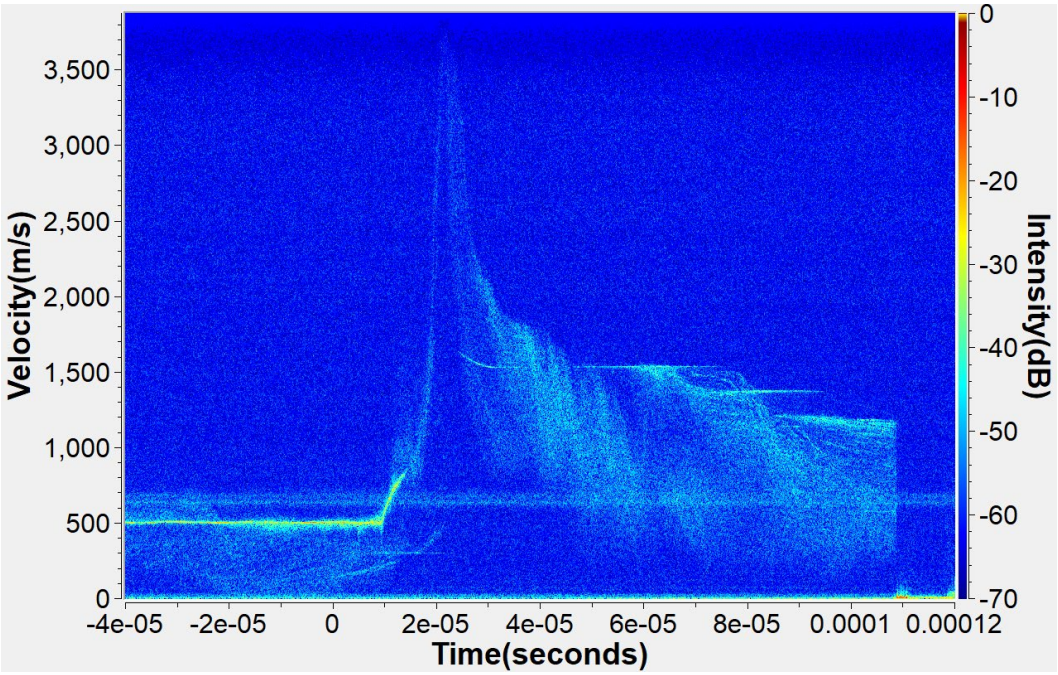

Fig. A-8 The PDV spectrogram from electrified DTE experiment E1 with an impact velocity of 505 m/s and a lead particle velocity of 1534 m/s

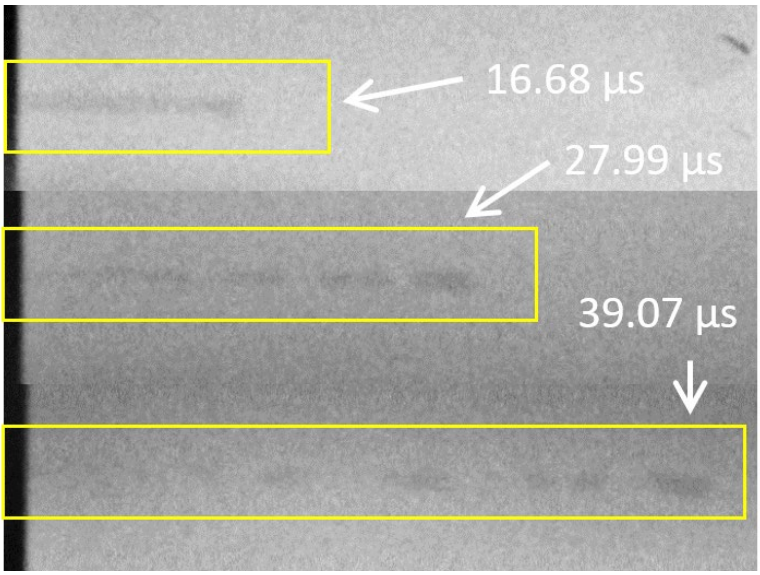

Fig. A-9 X-ray images of electrified DTE experiment E1. Times are measured relative to impact.

List of Symbols, Abbreviations, and Acronyms

Al	aluminum
ARL	Army Research Laboratory
Cu	copper
DEVCOM	US Army Combat Capabilities Development Command
DTE	dynamic tensile extrusion
EF	Experimental Facility
ET	electrothermal
HS	high speed
LRC	inductance, resistance, and capacitance
PDV	photon Doppler velocimetry
Zr	zirconium

1 (PDF) DEFENSE TECHNICAL INFORMATION CTR DTIC OCA

1 (PDF) DEVCOM ARL FCDD RLD DCI TECH LIB

11 (PDF) DEVCOM ARL FCDD RLW C P BARTKOWSKI FCDD RLW T R FRANCART FCDD RLW TA S BILYK P BERNING M COPPINGER W UHLIG B WILMER C ADAMS R BORYS JR FCDD RLW TD R DONEY M ZELLNER